

Finite element modelling of crackable connecting rods at fracture splitting process


T. Ozdemir*, S. O. Eruslu**

*Balıkesir University, Department of Mechanical Engineering, 10100 Balıkesir, Turkey,

E-mail: tozdemir1@gmail.com

**Namık Kemal University, Department of Mechanical Engineering, 59100 Tekirdağ, Turkey,

E-mail: oeruslu@nku.edu.tr

 <http://dx.doi.org/10.5755/j01.mech.21.2.7748>

1. Introduction

An engine connecting rod is dynamic component of engine therefore considered as a key component in terms of the structural durability and efficiency of an engine. In 1980s, the weight reduction of connecting rods are performed with optimisation approaches and some studies focused on the yielding and fatigue failure of connecting rods [1].

In operation, the connecting rod is subjected to dynamic inertia loads it must be adequately rigid and light in weight as well. Connecting rods cap ends were produced separately and had been sawn or machined apartly to enable of a bearing and attachment to the crankshaft. Traditional production methods are limited by the producing of the crackable PF (powder forged) connecting rod cap ends [2].

Fracture splitting is an alternative processing technique with low cost and high quality for production of connecting rods with the recent introduction of new splittable steels [3]. One of the desired factor in fracture splitting is minimum distortion at splitted cap end which is obtained by densely pearlitic microstructure of steels [4], [5].

The material ductility must be decreased for using splitting of end caps, this is achieved by decreasing Mn ratio and increasing V ratio on C70S6 perlitic steels [6]. Another important factor on fracture splitting is starting notches. German Manufacturers was found optimum notch depth 0.4-0.6 mm at experiments of Jetta Car Connecting rods [6]. Notch symmetry, notch size and notch shape are important for splitting process [7]. Notches are located at the approximate center of each of opposing positions on an inner surface of a crank pin opening.

At fracture splitting experiments pressure speed and fracture pressure must be chosen carefully to prevent ductile fracture and excessive deformation. Fracture apparatus is designed to meet these design criterias [6 - 8].

Fatigue strength of connecting rods under recycling loads and fretting corrosion because of the frictional contact faces must be considered at the design stage [9, 10]. Many studies on metallographic examinations and numerical analysis of connecting rods were presented in the literature. Numerical analysis was generally focused on finite element modelling of connecting rods. Two and three dimensional finite element modelling techniques are used to improve design by time and cost reduction. Webster and coworkers were developed three dimensional finite element model to study the effects of loading and boundary

conditions on connecting rods [11]. Stress-time history generations by dynamic stress analysis as function of crank angle is discussed by Majidpour et al [12]. Kubata et al. were used Ls Dyna explicit finite element code for understanding the distortion behaviour of connecting rod under impulsive split load [13]. Ozdemir T. were used LsDyna explicit finite element code to predict the cleavage time of C70S6 connecting rods [14]. Wang et al. were studied crack initiation in fracture splitting of connecting rods by using J integral technique [15]. They used three dimensional finite element models for validation of tensile fracture tests.

In our study fracture parameters were evaluated at the light of the previous works for C70S6 perlitic crackable steels. Dynamic crack propagation analysis of connecting rods with different microstructures were obtained by two dimensional finite element model. Linear Elastic Fracture Mechanics (LEFM) approaches were used because of the brittle manner of materials. Remeshing algorithm was developed for dynamic fracture analysis of connecting rods, which is commonly used for new crack tip position and optimize the element size [16, 17]. Fracture toughness values were found by using J integral technique. Cleavage behaviour and cleavage time of material was detected with the Charpy impact toughness.

2. Effective fracture parameters

Fracture parameters determined from experimental study on C70S6 steel [5] were used in numerical analysis. Starting notch was 0.4 mm at the experiments. It is recommended between 0.3 - 0.5 mm for brittle failure [6]. Pressure velocity in the connecting rod head section was 300 mm/s according to experimental data. Pressure velocity used in fracture splitting must be higher than 100 mm/s to avoid ductile fracture conditions [6]. Pressure velocity was defined as initial condition in finite element model.

The cracker apparatus was conic-shaped and becomes larger than the inner diameter of the connecting rod shank section as the tool penetrates in (Fig. 1). Resultantly, all the stress created by the hydraulic press on the cracker tool was dispersed along the connecting rod head section's inner diameter wall [16].

Pressure value at rod head section was computed as 3070 MPa from conic section calculations in Eq. 1 [18]:

$$P_{rod} = \frac{F_{press} \cos \rho}{\pi D_{ave} L_{con} \sin\left(\rho + \frac{\alpha}{2}\right)}, \quad (1)$$

here F_{press} is force of the press applied. In our analysis $F_{press} = 1600$ kN, ρ is friction angle for $\mu = 0.2$, D_{ave} , L_{con} , $a/2$ is average diameter, length of conic section and conical angle respectively seen in Fig. 1, here average diameter is expressed as:

$$D_{ave} = \frac{D_{ex} + D_{in}}{2} \quad (2)$$

Apparatus dimensional values are given as follows:

$$D = 22 \text{ mm}, L = 28 \text{ mm}, \frac{\alpha}{2} = 4.$$

The connecting rod was restraint at x direction with the developed apparatus seen in Figs. 2 and 3. At this

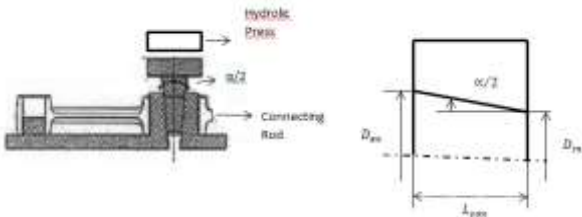


Fig. 1 Fracture splitting process [15] and conic section detail



Fig. 2 Fracture splitting apparatus



Fig. 3 Cracker tool equipped with hydraulic press [5, 15]

apparatus uniform pressure at the head section was applied to crack tip and crack face pressure was obtained. The boundary conditions used in finite element model was established according to this cracker tool process.

3. Fracture toughness criteria

Charpy impact toughness K_{IC} for each microstructures were used for validation of crack propagation. Charpy impact toughness values were calculated from charpy impact energy by using J integral on the crack length Δa expressed as below [19]. Charpy impact energy and fracture toughness are given in Table 1:

$$J = C \Delta a^p \quad (3)$$

here C is compliance is defined by geometry of charpy specimen (a_0, B_0, w) as follows:

$$C = \left(\frac{2}{p}\right)^p \frac{\eta(a_0)}{B_0 (w - a_0)^{p+1}} W_t^p W_m^{1-p}, \quad (4)$$

where W_t is entire fracture energy, W_m is state energy achieved at maximum force, p and $\eta(a)$ are parameters defined by:

$$p = \frac{3}{4} \left(1 + \frac{W_m}{W_t}\right)^{-1}, \quad (5)$$

$$\eta(a) = 13.81(a/w) - 25.12(a/w)^2, \quad (6)$$

here $\frac{W_m}{W_t} = n$, n is strain hardening coefficient approximately equal to ductility A_f according to Kraft et al. [20]. Strain hardening coefficient n is taken 0.19 in our analysis [21].

$$J = \left(\frac{2}{p}\right)^p \frac{\eta(a_0)}{B_0 (w - a_0)^{p+1}} W_t A_f^{1-p} \Delta a^p, \quad (7)$$

here $W_t = KV$ KV is impact energy.

Table 1
Charpy impact properties of connecting rod steel with different microstructures [8, 22]

Microstructure	Charpy Impact Energy, J	Charpy Impact Toughness, MPa m ^{1/2}
Perlitic	8	33.389
Tempered Martensitic	10	37.330
Upper Bainitic	9	35.415

For plane strain conditions fracture toughness can be defined as follows:

$$K_{IC} = \left(J \frac{E}{(1-\nu^2)} \right)^{0.5}. \quad (8)$$

According to Irwin's approach dynamic stress intensity factor is always equal to dynamic fracture toughness [16].

In our work effective stresses at crack face is shear stresses so Mode II stress intensity calculation was performed according to strain energy release rate G defined as below:

$$G = K_{II}^2 \left(\frac{1-\nu^2}{E} \right) \quad (9)$$

and dynamic fracture toughness defined as follow:

$$K_{IIa}(\dot{a}, a(t)) = K_{IC}(\dot{a}, a(t)), \quad (10)$$

here $K_{IIa}(\dot{a}, a(t))$ is dynamic stress intensity factor for Mode II loading, \dot{a} is crack tip velocity, a is crack length.

Dynamic crack propagation was detected according to following equation:

$$K_{IIa}(\dot{a}, a(t)) \gg K_{IC}(0, a(t)) \quad (11)$$

Variation of charpy impact toughness values were obtained by direct proportion with calculated static stress intensity factor according to crack length at finite element model (FEM).

Dynamic stress intensity factor was computed at crack tip for every time increment Δt , crack tip velocity was predicted by FEM analysis.

4. Finite element modelling for dynamic crack propagation

Dynamic crack propagation were studied by using two dimensional finite element model. Only quarter half of the connecting rod was modelled because of the symmetry. Quadratic isoparametric eight node (Ansys 12.0 Plane 183) elements were used for two dimensional plane strain analysis. Symmetry boundary conditions and uniform pressure were applied seen in Fig. 4. The outside circle of the modelled ring were restrained in horizontal direction x according to fracture conditions used in experiments seen in Figs. 2-3. Convergence study was performed with singular elements at the cracktip region in Fig. 5. This study was aimed to find appropriate mesh density in the model. It is seen from figure that stress intensity factor calculations at the cracktip is not changed significantly with increasing number of elements between 3000 to 5000. According to approximation results of study 3000 element was used at the finite element modelling of ring. Transient dynamic analysis and Newmark scheme was performed.

Remeshing technique was used for mesh generation at each step. Dynamic stress intensity factor and crack tip velocity was computed at every time increment. New crack tip position was found by calculation of $(\dot{a} \Delta t)$. The modeled crack was open at the initial stage of calculations because of the recommended starting notch for brittle failure to avoid ductile fracture at fracture splitting process.

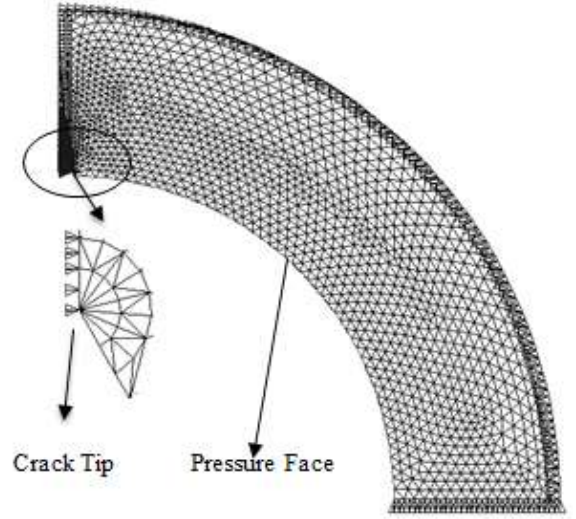


Fig. 4 Finite element modelling of connecting rod

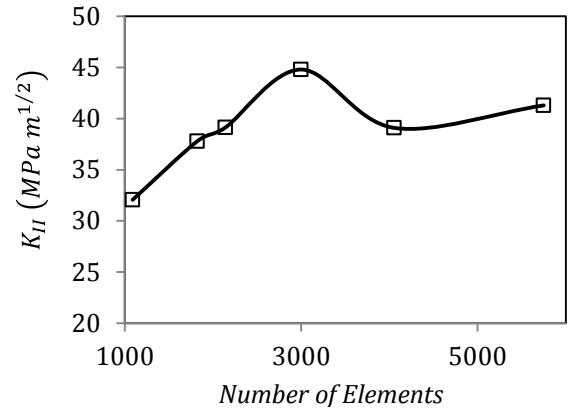


Fig. 5 Convergence study of finite element model

5. Theoretical definition of model

In our analysis it was found that compressive and shear stresses were developed at the crack face under the boundary conditions presented in Fig. 4. Mixed Mode stress intensity calculation was performed. Stress field is given by [23]:

$$\begin{bmatrix} \sigma_{xx} \\ \sigma_{yy} \\ \tau_{xy} \end{bmatrix} = \frac{K_I}{\sqrt{2\pi r}} \cos \frac{\theta}{2} \begin{bmatrix} 1 - \sin \frac{\theta}{2} \sin \frac{3\theta}{2} \\ 1 + \sin \frac{\theta}{2} \sin \frac{3\theta}{2} \\ \sin \frac{\theta}{2} \cos \frac{3\theta}{2} \end{bmatrix} + \frac{K_{II}}{\sqrt{2\pi r}} \begin{bmatrix} -\sin \frac{\theta}{2} \left(2 + \cos \frac{\theta}{2} \cos \frac{3\theta}{2} \right) \\ \sin \frac{\theta}{2} \cos \frac{\theta}{2} \cos \frac{3\theta}{2} \\ \cos \frac{\theta}{2} \left(1 - \sin \frac{\theta}{2} \sin \frac{3\theta}{2} \right) \end{bmatrix}, \quad (12)$$

here θ and r are local coordinates at the crack tip seen in Fig. 6.

$$K_{II} = \tau_{xy} \sqrt{\pi a} Y \quad (13)$$

here τ_{xy} is shear stresses is calculated according to Eq. (10). Y is geometrical correction factor, it was taken 1.2 from reference for initially cracked cylinder under internal pressure [24]. Static stress intensity factor variation with crack length calculated from Fem analysis was compared with the analytic results in Fig. 7. Static stress intensity factor results obtained by fem were good agreement with analytic results. At compressive stresses crack propagation wasn't obtained [25]. Mode I calculation was not take into account for crack propagation in our study. Mode II stress intensity calculation was performed in Eq. (12) because of the shear stress on crack face.

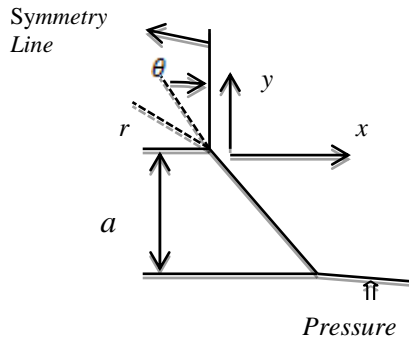


Fig. 6 Connecting rod head section crack tip scheme

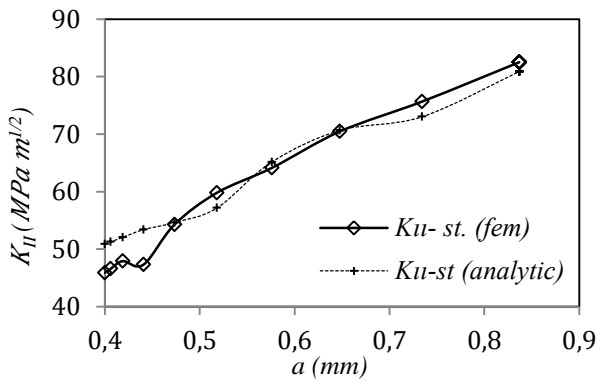


Fig. 7 Comparison of static stress intensity results

6. Results and discussion

Numerical results were found from finite element analysis were presented at this section. Variation of dynamic stress intensity factor for different microstructures are given in Fig. 8. It is shown in figure that steels cleavage times of steels are between 350 - 670 μ s.

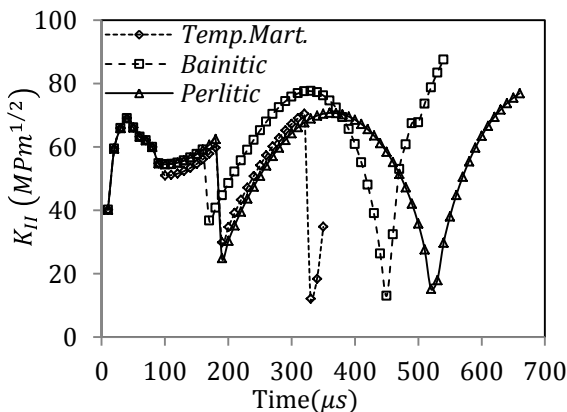


Fig. 8 Dynamic stress intensity factor vs. time

In Fig. 9 dynamic stress intensity factor and fracture toughness variation according to fracture toughness criteria is shown for tempered martensitic steel. Crack arrest time and crack arrest lengths were obtained in Table 2. It is seen from figures and table all steels arrest times

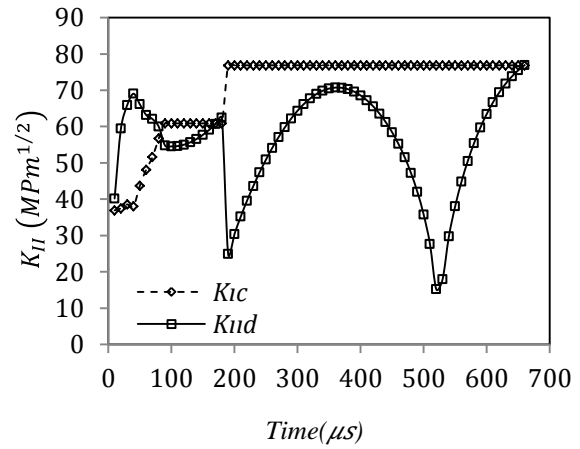


Fig. 9 Dynamic stress intensity factor and fracture toughness comparison

Table 2

Predicted crack propagation results			
C70S6 Steel	Arrest time, μ s	Crack arrest length, mm	Cleavage time, μ s
Perlitic	190	3.327	380
Tempered martensitic	190	3.136	670
Bainitic	170	2.412	550

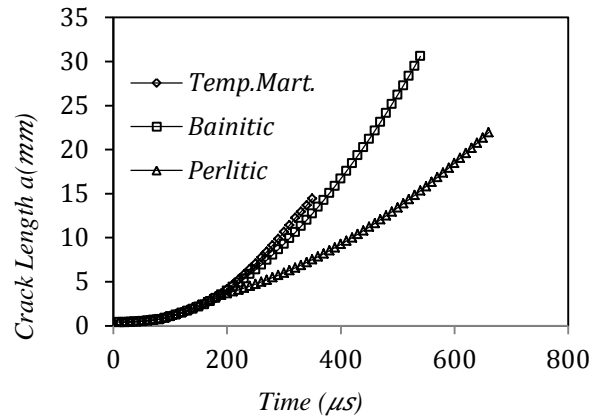


Fig. 10 History of crack extension for C70S6 steels

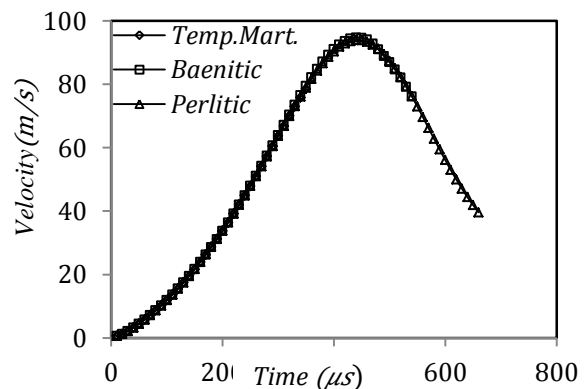


Fig. 11 History of cracktip velocity for C70S6 steels

and arrest lengths are predicted closer each other. In Figs. 10 - 11 time dependent crack length and cracktip velocity is shown. Fracture parameters used in experiments are given brittle failure conditions with initial velocity. In Fig. 12 applied mesh details and crack tip propagation is given for C70S6 perlitic steels.

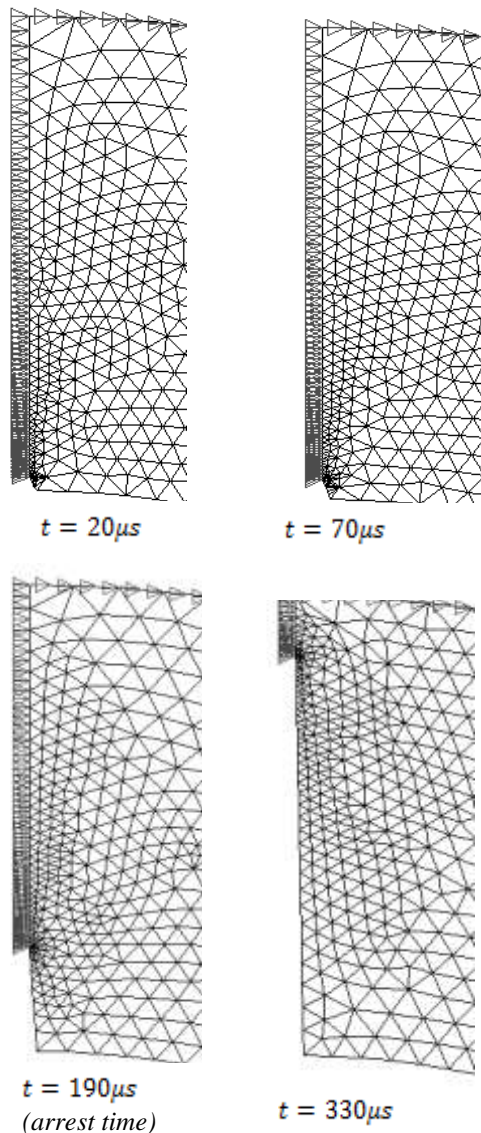


Fig. 12 Dynamic crack propagation with remeshing layout

7. Conclusions

In this study dynamic crack propagation of fracture splitted connecting rods with different microstructures are investigated. Traditional perlitic steels, tempered martensitic and bainitic steels are studied. Crack propagation, crack arrest times, cleavage times are found for each microstructure numerically. Dynamic crack propagation with the detection of fracture toughness criteria is predicted brittle failure with initial velocity. Shear stress effective stress intensity factor calculations are in good agreement with predicted results by finite element model. It is seen that remeshing technique may be applicable for fracture splitting process.

References

1. Lee, M.K.; Lee, H.; Lee, T.S.; Jang, H. 2010. Buckling sensitivity of a connecting rod to the shank sectional area reduction, *Mater Des* 31: 2796-2803. <http://dx.doi.org/10.1016/j.matdes.2010.01.010>.
2. James, R.D. 2005. Connecting rod evaluation. Metal Powder Industries Federation, Princeton. Available from Internet: <http://www.pickpim.com/designcenter/Conrod.pdf>.
4. Aksoy, Z.; Özdemir, Z.; Özdemir, T. 2012. A metallographic examination of fracture splitting C70S6 steel used in connecting rods, *Marmara Univ. Fen Bil. Derg*, 24(2): 45-58.
5. Corus Engineering Steels. 2003. An improved machinable air cooled fracture splittable carbon steel for connecting rods. Available from Internet: http://www.tatasteelautomotive.com/file_source/automotive/Publications/fractim.pdf.
6. Özdemir, Z. 2013. Biyel Kolu Başlığının Kırma Yöntemi ile İmalatında Kırma Parametrelerinin Optimizasyonu. Balıkesir Üniversitesi, PhD. Thesis.
7. Gu, Z.; Yang, S.; Ku, S.; Zhao, Y.; Dai, X. 2005. Fracture splitting technology of automobile engine connecting rod, *Int J Adv Manuf* 25: 883-887. <http://dx.doi.org/10.1007/s00170-003-2022-2>.
8. Aksoy, Z.; Özdemir, Z.; Özdemir, T. 2012. A study on fracture parameters of crackable connecting rods. *Sakarya Univ. Fen Bil. Derg* 16(2): 113-122.
9. Momose, Y.; Ota, S.; Yamamoto, T. 2005. Method of and apparatus for cracking connecting rod. US Patent.
10. Hye, K.; Tae, K.; Tai, J.; Hyun, C.; Kim, S.J.H. 2010. Fatigue characteristics of high strength C70S6 and SMA40 steels. *Materials Science and Engineering* 527: 2813-2818. <http://dx.doi.org/10.1016/j.msea.2010.01.039>.
11. Pravardhan, S.; Fatemi, A. 2005. Connecting rod optimization for weight and cost reduction. *Sae International* 987: 1-8.
12. Webster, W.D.; Coffell, R.; Alfaro, D. 1983. A three dimensional finite element analysis of a high speed diesel engine connecting rod, *SAE Technical Paper* 831322: 83-96.
13. Majidpour, M.; Shakeri, M.; Akhlaghi, M. 2002. Quasi-dynamic stress analysis of connecting rod and cyclic stress-time histories generations. The Second International Conference on Internal Combustion Engines.
14. Tsuyoshi, K.; Shinya, I.; Tsuneo, I.; Toshikatsu, K. 2007. Development of fracture splitting method for Case hardened connecting rods. Advance Technology Research Div. Research and Development Yamaha Technical Paper.
15. Özdemir, T. 2013. Motor biyel kolunun baş kısmının kırılmasının sonlu elemanlar yöntemiyle numeric analizi üzerine bir çalışma. Balıkesir Üniversitesi PhD Thesis.
16. Wang, Y.; Kou, S.; Jin, W. 2007. Determination and application of critical *J* integral for C70S6 in fracture splitting connecting rod. International Conference on Mechanical Engineering and Mechanics.
17. Shahani, A.R.; Fasakhodi, A.M.R. 2009. Finite element analysis of dynamic crack propagation using remeshing technique, *Mater Des* 30: 1032-1041.

- <http://dx.doi.org/10.1016/j.matdes.2008.06.049>.
18. **Bouchar d, P.O.; Bay, F.; Chastel, Y.; Toven a, I.** 2000. Crack propagation modelling using an advanced remeshing technique, *Comput Methods Appl Mechan Eng* 189: 723-42.
[http://dx.doi.org/10.1016/S0045-7825\(99\)00324-2](http://dx.doi.org/10.1016/S0045-7825(99)00324-2).
 19. **Kutay, M.G.** 2010. Göbek mil bağlantıları. Available from Internet: http://www.guven-kutay.ch/ozet-konular/09_GobekMil.pdf.
 20. **Strnadel, B.; Matocha, K.** 2009. Testing samples size effect on toughness of structural steels, *Metalurgija* 48(4): 253-256.
 21. **Kraft, J.M.** 1964. Correlation of plane strain toughness with strain-hardening characteristics of a low, medium, and a high strength steel, *Applied Materials Research* 3: 88-101.
 22. **Afzal, A.** 2004. Fatigue behavior and life predictions of forged steel and powder metal connecting rods, University of Toledo College of Engineering Master Thesis.
 23. **Bhadeshia, H.K.D.H.** 1997. Martensite and bainite in steels: transformation mechanism and mechanical properties, *J. Phys. IV France* 7, C5 - 367.
<http://dx.doi.org/10.1051/jp4:1997558>.
 24. **Saouma, V.E.** Lecture Notes in Fracture Mechanics. Available from Internet: <http://ceae.colorado.edu/~saouma/Lecture-Notes/lecfrac.pdf>.
 25. **Saleh, N.A.H.** 2012. A study on second mode stress intensity factor (KII) of cracked plates under compression load, *Basrah Journal for Engineering Science*: 54-65.
 26. Air Force Materials Laboratory Technical Report. 1974. Two Dimensional stress intensity factor solutions for radially cracked rings. Available from Internet: <http://www.dtic.mil/get-tr-doc/pdf?AD=ADA 018670>.

T. Ozdemir, S.O. Eruslu

FINITE ELEMENT MODELLING OF CRACKABLE CONNECTING RODS AT FRACTURE SPLITTING PROCESS

S u m m a r y

In this study crack propagation analysis of impulsively loaded connecting rods with different microstructures namely perlitic, bainitic, tempered martensitic were studied numerically for evaluation of fracture parameters. Fracture splitting parameters in experiments for uniform impact force distribution was concerned in numerical analysis. Brittle crack propagation at starting notches was obtained by impulsive load. Dynamic crack propagation was studied by using two dimensional finite element model and crack tip positions were determined by remeshing algorithm. Dynamic stress intensity factors were calculated by J integral technique and cleavage failure was detected according to dynamic fracture toughness parameters by instrumented Charpy impact test. Crack propagation, crack arrest times, cleavage times were found and compared numerically for three different microstructures. Predicted shear effective stress intensity calculations, crack tip velocity, crack extension results are found supplementary data for experimental fracture parameter optimisation.

Keywords: Dynamic crack propagation, connecting rods, fracture splitting, fracture parameters, *J* integral.

Received August 14, 2014

Accepted March 12, 2015